Outstanding problems in the band structures of ^{152}Sm

J. B. Gupta and J. H. Hamilton

Phys. Rev. C **96**, 034321 — Published 22 September 2017

DOI: 10.1103/PhysRevC.96.034321

Outstanding problems in the band structures of ^{152}Sm

J.B. Gupta[1] and J.H. Hamilton[2]

[1]Ramjas College, University of Delhi, Delhi-110007, India
[2]Physics Department, Vanderbilt University, Nashville, TN, 27235, U.S.A.

Received June 6, 2017, revised July 20, 2017

The recent data on *B*(E2) values, deduced from the multi-Coulex excitation of the low spin states, in the decay of ^{152}Sm, and other experimental findings in the last two decades are compared with the predictions from the microscopic dynamic pairing plus quadrupole model of Kumar-Baranger. The 1292.8 keV 2^+ state is assigned to the 0_3^+ band and K=2 assignment of 1769 keV 2^+ state is confirmed. The anomaly of the shape coexistence of the assumed spherical β-band versus the deformed ground band is resolved. The values from the critical point symmetry X(5) support the collective character of the β-band.. The problem with the two term Interacting Boson model Hamiltonian in predicting β-, and γ-band in ^{152}Sm lead to interesting consequences. The collective features of the second excited $K^\pi = 0_3^+$ band are preferred over the "pairing isomer" view. Also the multi-phonon nature of the higher lying $K^\pi = 2_2^+$ βγ band and $K^\pi = 4^+$ band are illustrated vis-a-vis the new data and the nuclear structure theory.

PACS numbers 21.60.Ev, 21.60.Cs, 21.10.Re, 27.70+q

Key words:
[NUCLEAR STRUCTUE, collective multiphonon bands, ^{152}Sm, microscopic theory]

I. **INTRODUCTION**

The softly deformed nucleus ^{152}Sm is one of the N=90 isotones, lying at the edge of the spherical to deformed transition path, which have been recently associated with the approximate analytical solution for the critical point symmetry X(5) [1], and was cited as the first example of an X(5) nucleus [2]. This nucleus has been studied in a number of works, in experiment and in theory and is still of current interest. The ground band (g-band), the $K^{\pi}=0_2^+$ β-band and the $K^{\pi}=2^+$ γ-band have been well established [3, 4]. While γ-g $E2$ transitions yielded consistent band mixing parameter Z_{γ}, the β-g $E2$ transitions did not yield a consistent Z_{β}. Hamilton *et al.* (1971) [5] studied the β-γ band mixing in ^{152}Sm to resolve this anomaly. In this approach, the β-γ band mixing was only a second order effect. In a careful γ-γ coincidence work with large volume Ge(Li) detectors, they noted the surprising value of $B(E2, 2_{\gamma}\rightarrow 2_{\beta}) = 0.13$ e^{2}b^2, of the 275 keV γ-ray peak, being greater than $B(E2, 2_{\gamma}\rightarrow 2_{g})$ by a factor of ≥2, indicating (unexpected) good mixing of the β, γ bands. However, they also noted that the $B(E2, 2_{\gamma}\rightarrow 0_{\beta})$, corresponding to a weak intensity 401 keV peak in the γ-ray singles spectrum, was almost zero. Also the $B(E2, 3_{\gamma}\rightarrow 2_{\beta})$ of the 423.45 keV was very weak [5] (~0.1 W.u). This was as expected, since the band mixing was only between the two spin $I^{\pi}=2^+$ states. These findings are important in relation to the *shape co-existence view of β-band and ground band*, arising from later works (1998) on this nucleus [6]. Earlier, the problem of the band mixing anomalies in this region, were resolved in the microscopic approach of the dynamic pairing plus quadrupole model of Kumar–Baranger [7] by Kumar in (1974) [8], where only the lower three K-bands were considered Here we will analyze all 8 K-bands in ^{152}Sm.

The advent of the interacting boson model (IBM) of Arima and Iachello [9] led to fresh studies of $^{146\text{-}154}$Sm isotopes by Scholten *et al*. (1978) [10], who reproduced the variation in the spectra with neutron number N by varying a single control parameter. The predictions in SU(3) symmetry (selection rules) in which the β, γ bands belong to the same SU(3) ($\lambda=N_B$-2, μ=2) multiplet [9], led to the prediction of strong γ-β transitions [6], instead of it being a second order effect in the Bohr-Mottelson (BM) geometrical frame work [5]. This led to intense experimental efforts to determine the absolute B(E2) values for β-g, γ-g and γ-β transitions, rather than only the B(E2) ratios.

Casten *et al*. (1998) [6] employed the OSIRIS cube array of Compton suppressed high efficiency Ge(Li) detectors, which enabled them to identify clearly the 401 keV γ-ray peak (which was hardly seen in the earlier works [5]), and to estimate the upper limit of its relative intensity I_γ. They noted that the branching ratio $R^{\gamma}_{0g}= B(E2;2_\gamma \rightarrow 0_\beta)/ B(E2;2_\gamma \rightarrow 0_g) = 0.048(4)$, is extraordinarily small. From the life time $T_{1/2}(2_\gamma)$ data they also deduced the absolute value of $B(E2;2_\gamma \rightarrow 0_\beta)$ =0.17 W.u. This was a surprising result [6], in IBM framework. Historically, it is rather interesting, that in the earlier studies [5], the strong $B(E2, 2_\gamma \rightarrow 2_\beta)$ =0.13 e^2b^2 (~27 W.u) was surprising, while in the post IBM works [6, 11 ,12], the weak $B(E2;2_\gamma \rightarrow 0_\beta) = 0.17$ W.u. is a surprise. This situation of IBM versus BM model is known, but needs further study.

Besides the lower three bands, the information on higher levels in ^{152}Sm listed in (National Nuclear Data Centre) nndc compilation [3, 4], can shed more light on its structure. The 0_3^+ at 1082.8 keV, along with a 2^+ level at 1292.8 keV, is listed, including the de-exciting γ-rays. A 4^+ level at 1612.9 keV [3] is a probable member of this band. The validity of calling it as a "pairing isomer" is studied in the present work. Higher 0^+ states at 1658.8 (weak decay to 2_β and 2_g, strong to 1^-) and 1755.0 keV (weak decay to 2_β) were known [3] from the reaction work and confirmed in later work [13]. A 2^+ level at 1769.1 keV and $I^\pi=3^+$ at 1907.7 keV are known [3,13]. From the recent multiple step Coulomb excitation [13], its $K^\pi=2^+$ assignment was suggested. Also a $K^\pi=4^+$ band with 8 members up to $I^\pi =11^+$ is listed in [3]. These experimental findings over the last two decades, offer a challenge for nuclear structure theories. In the present work, we analyze the latest data in ^{152}Sm, with the dynamic PPQ model predictions, and thus supplement and extend the earlier studies in [8] and [14]. We also study these issues in the IBM, which provides a highly successful alternate framework [9]. We also try to explore the band mixing anomalies of BM model versus IBM. The multiphonon character of the $K^\pi=2_2^+$ βγ band and of $K^\pi = 4^+$ band in ^{152}Sm are studied.

In Sec. II, brief outlines of the dynamic PPQ model and the IBM are given. In Sec. III, the results of the microscopic theory and IBM-1 are compared with data. In Sec. IV empirical results on ground, γ- and β-band in N=90 isotones are illustrated. In Sec. V summary of our work is given and the above stated anomalies are reviewed.

For the first time we have realized the limitation of the SU(3) symmetry breaking term by EPS n_d in IBM. The subtle difference between the SU(3) symmetry in IBM frame work and the Rotor model features in the shape transitional nucleus is also pointed out here for the first time. We stress that the description of the nucleus ^{152}Sm is a very important problem that has not been solved up to now. Two interesting ideas have been formulated before concerning ^{152}Sm: shape coexistence and pairing isomer, and the analysis presented in this manuscript shows that both ideas do not work in the case of ^{152}Sm.

Finally, we emphasize that the results of calculations based on the Kumar-Baranger approach and presented here show how important a deformation dependence of the components of the inertia tensor is for the description of the properties of the collective states. Kumar had emphasized in his works this aspect of nuclear structure often, and this continues an important ingredient in the growth of collectivity.

II. THEORY

A. Dynamic pairing plus quadrupole model

The dynamic pairing plus quadrupole (DPPQ) model employs a mean field, represented by harmonic oscillator potential, and the residual long range quadrupole force and short range pairing interaction. In the Kumar-Baranger approach, quadrupole interaction and pairing are treated at the same footing, in the Hartree Bogoliubov Technique (HBT) [7]. The valence nucleon space includes two major oscillator shells of 21 protons and 28 neutrons. Several improvements were made in the treatment of the model, as discussed in Ref. [8]. The dynamic PPQ model has been found useful especially for the shape transitional nuclei. Besides the mean field produced by all the valence nucleons, the PPQ Hamiltonian includes the long range, deformation producing residual quadrupole interaction term, and the short range pairing interaction term (Eq. 1)

$$H_{PPQ} = H_{sph} + H_Q + H_P. \quad (1)$$

Using the global parameters of spherical single particle energies ε_α for the n=4, 5 oscillator shells for protons and the n=5, 6 shells for neutrons, and using appropriate

quadrupole force $\chi = X \times A^{-1.4}$ and the monopole pairing strengths g_p, g_n, we deduced the parameters of the collective Hamiltonian from H_{PPQ}

$$H_{coll} = V(\beta, \gamma) + T_{vib}(\beta, \gamma) + T_{rot}(\beta, \gamma), \quad (2)$$

where $T_{vib}(\beta,\gamma) = \frac{1}{2} B_{\beta\beta}(\partial\beta/\partial t)^2 + B_{\beta\gamma}\beta(\partial\beta/\partial t)(\partial\gamma/\partial t) + \frac{1}{2} B_{\gamma\gamma}(\beta\partial\gamma/\partial t)^2$ (3)

and $T_{rot}(\beta,\gamma) = \frac{1}{2} \Sigma_k \theta_k(\beta, \gamma) (\hbar\omega_k)^2$. (4)

As described in detail in Ref. [7, 8], no fixed shape is assumed for the nucleus, and it has full freedom on the (β, γ) space (β=0 – 0.5, γ=0°-60°) for every spin state, and finds its own equilibrium shape. Summation over a mesh of 92 points provides the dynamics of the Hamiltonian. Also the kinetic coefficients B's and the moments of inertia θ_k are allowed to vary over the full (β, γ) space. This provides the full dynamics of the H_{coll}.

All the input parameters are kept fixed for the whole region. But minor variation (few percent) in the strength of quadrupole force constant $\chi = X \times A^{-1.4}$ is allowed to adjust the energy scale. Also all the kinetic coefficients are multiplied by a renormalization factor F_B, to compensate for the inert nuclear core (Z=40, N=70 closed shells) effects. For ^{152}Sm, we set the quadrupole strength factor at X=70.0 (a regional value) and the core re-normalization factor F_B at 2.2 (close to the regional value of 2.4) for the kinetic coefficients Bs and the moments of inertia θ_k in Eqs. (3, 4). Also the charge parameter e_n =0.65, e_p(=1+e_n) for the electromagnetic operators, is close to the regional value. See Ref. [7, 8] for more details.

B. Interacting boson model

In the algebraic group theoretical model of sd-IBM of Arima and Iachello [9], the collective structure of atomic nuclei is described in terms of the L=0 s-bosons and L=2 d-bosons, which represent the correlated valence nucleon pairs. In IBM-1, no distinction is made between the neutron and proton bosons. The conservation of boson number N_B in boson-boson interaction leads to the U(6) group algebra, with 3 dynamical chains. The quantum numbers associated with the subgroups define the IBM Hamiltonian. The three limiting symmetries are labeled as U(5), SU(3) and O(6), which are related to the spherical vibrator, deformed rotor and γ-unstable rotor respectively of the BM model. A 4-term Hamiltonian in (multipole) MULT form [9]

$$H_{IBM} = \varepsilon\, n_d + kQ\cdot Q + k'L\cdot L + k''P\cdot P \qquad (5)$$

is often used for deriving the eigenvalues and the B(E2) values. However, for studying the dependence of the shape phase transition with varying neutron number *N* on the IBM parameters, it is useful to limit to the 2-term Hamiltonian, in order to minimize the number of free parameters and to get a better insight of the role of the IBM parameters [6, 12]. The 2-term IBM-1 Hamiltonian can be written as (*k* positive)

$$H_{IBM} = \varepsilon\, n_d - kQ\cdot Q = k(\varepsilon/k\, n_d - Q\cdot Q). \qquad (6)$$

Here, $n_d = d^+d$ counts d-bosons and ε is the boson energy, Q is the quadrupole operator:

$$Q= (d^+s + s^+d) + \chi[d^+d]^{(2)}. \qquad (7)$$

We have used the computer codes PHINT and FBEM of Scholten [15].

Though IBM is based on the shell model, but the parameters of H_{IBM} have to be deduced from a fit to the experimental data of level energies (and possibly certain B(E2) values). Chou *et al*. (1997) [16] did a detailed study of the effect of pair of IBM-1 parameters and boson number N_B, on the nuclear structure of some 145 nuclei in the A=120-200 mass region, in search of some guidance on the selection of the parameters. Casten *et al*. [6] adopted the same method for ^{152}Sm. Keeping the scaling parameter *k* constant they varied ε and χ and obtained contours for fixed values of *k*. Here, for ^{152}Sm, an axially symmetric soft deformed nucleus, we fix χ= -1.32 (a deformed rotor value), and vary ε and *k*. To vary ε/*k*, one can keep *k* fixed and vary boson energy ε. Since this yields varying energy scales, we varied ε for different *k* values, to reproduce $E(2_g)$ in each case. The results of our evaluation are given in Sec. IIIA and IIID.

III. RESULTS FROM DPPQM and IBM

A. Shape co existence anomaly

To analyze the cause of small strength of ($2_\gamma \rightarrow 0_\beta$) transition, Casten *et al*. [6] varied the control parameter (ε/*k*) in IBM Hamiltonian (Eq. 6). They noted that, the value of $R^{\gamma}_{0g} = B(E2; 2_\gamma \rightarrow 0_\beta)/B(E2;2_\gamma \rightarrow 0_g)$, calculated in the interacting boson model (IBM) [9], goes to zero extremely rapidly with the variation of the controlling parameter ε/*k*, changing by orders of magnitude for a narrow range of parameter values [6]. It was used for the selection of ε/*k* value for ^{152}Sm. They reasoned that such small transition

strength may arise, if one regards the state 2_γ as part of the 2-phonon triplet based on the spherical (zero phonon) 0_β state, with 2_β as the 1-phonon state. They suggested that the spherical 0_β^+ state *co-exists* with the deformed ground band.

Iachello *et al*. [11] deduced the wave amplitude versus $n_{d,}$ boson number distribution (in the SU(5) basis) in IBM-1, and noted the large amplitude for 0_β state of ^{152}Sm (at $n_d = 0 - 1$), similar to the ground state of spherical ^{150}Sm. Zamfir *et al.* (1999) [12] performed very high statistics measurement and corrected several absolute B(E2) values. They noted the energy pattern of a possible two phonon triplet formed on the 0_β state and found some features leading to the shape co-existence view. The smaller energy ratio $R_{4/2}$=E(4-2)/E(2-0) =2.69 for the β-band spacing, compared to 3.01 for ground band clearly suggests it [12]. This proposition was further supported by the increased 2n transfer cross section σ(t, p) strength for excited 0^+ states, observed in Ref. [17]. However, Zamfir *et al.* [12] also noted several inconsistencies in such an extreme proposition.

Fig.1 depicts the partial energy spectrum of ^{152}Sm [3]. Indeed, if one looks at the horizontal layout of energy levels, a 2-phonon triplet (4_2^+, 2_3^+, 0_3^+) of levels is clearly seen over the zero phonon 0_2^+ base and 1-phonon 2_2^+ level. So that, the suggestion of a shape co-existence, had a good starting basis. But if one looks at the vertical patterns, the rotational *K*-bands may also be seen. The choice may also depend on the relations between the collective states, along with the level pattern (see below).

B. Energy spectrum and *K*-components from DPPQ model

Firstly, we look at the predictions from the dynamic PPQ model. The level energies in ^{152}Sm from DPPQ model are compared with experiment in Table I. Also the partial energy level spectrum is illustrated in Fig. 2. The energy scale for the excited bands is rather expanded, a typical feature of the present set up of the model. However, the basic pattern is well reproduced, including the apparent two phonon triplet of ($4_{\beta,}$ 2_γ and 0_3^+). The 2γ phonon (K=0_4^+, $2_{K=2} = 2_{\beta\gamma}$, $4_{K=4}$) combinations of the states, possible in the collective model and seen in experiment, are also predicted in the same order in

DPPQM (Fig. 2). The fifth 0_5^+ in DPPQ model (Table I) may be associated with the 1755 keV state.

TABLE I. The energy level spectrum (keV) of ^{152}Sm and the DPPQ model predictions.

Band		0^+	2^+	3^+	4^+	5^+	6^+
$K^\pi=0_1^+$	Exp	0	121.8		366.5		706.9
	DPPQ	0	121.3		361		687
$K^\pi=0_2^+$	Exp	684.8	810.5		1023.0		1310.5
	DPPQ	1003	1212		1449		1730
$K^\pi=2_1^+$	Exp		1085.8	1233.9	1371.7	1559.6	1728.3
	DPPQ		1556	1718	1885	2073	2288
$K^\pi=0_3^+$	Exp	1082.8	1292.8		1612.9		2004.2
	DPPQ	1750	2111		2360		2668
$K^\pi=2_2^+$	Exp		1769.1	1907.7			
	DPPQ		2660	2936			
$K^\pi=4_1^+$	Exp				1757.0	1891.1	2040.1
	DPPQ				2947	3244	3441
$K^\pi=0_4^+$	Exp	1658.8					
	DPPQ	2864	3218				
$K^\pi=0_5^+$	Exp	1755.0					
	DPPQ	3026					

TABLE II. *K*-components in $I^\pi=2^+$ states of ^{152}Sm from DPPQM, and β_{rms} and γ_{rms}.

	2_g^+	2_β^+	2_γ^+	2_{03}^+	$2_{\beta\gamma}^+$
E(keV)	121.8	810.5	1085.8	1292.8	1769.1
K=0	99.89	97.98	3.05	92.18	10.74
K=2	0.11	2.02	96.95	7.82	89.26
β_{rms}	0.265	0.307	0.257	0.290	0.268
γ_{rms}	14.3°	10.9°	22.5°	8.3°	18.6°
E (PPQ)	121	1212	1555	2111	2660

The predominant *K*-component in the *K*-admixture of a collective state helps to identify its *K*-band character. The predicted *K*-components for ^{152}Sm from dynamic PPQ model calculations are listed in Table II. The spin *I*=2 states of ground and β-bands are almost pure $K^\pi=0^+$, and the γ-band has 97% $K^\pi=2^+$ predominance. The higher 2_{03}^+ state also has only ~8% *K*=2 admixture. The fifth *I*=2 state at 1769.1 keV, in DPPQ model has predominant (89%) $K^\pi=2^+$ component. The fifth *I*=4 state at 1757 keV has (7+25+68)%

K=0,2,4 components. The *K*-components of the states of higher spin members of the excited bands also display a similar pattern.

The β_{rms} and γ_{rms} are deduced from the summation of β^2 and $\beta^3\cos3\gamma$ functions dependence upon the spread of the wave function in the (β,γ) space. The numbers indicate slightly larger dynamic fluctuations (softness) in β degree of freedom for the β-band and the over all stability across different *K*-bands. The same is indicated by the fluctuations in the γ-degree of freedom for $K^{\pi}=2_1^+$ and $K^{\pi}=2_2^+$ bands.

C. Potential energy surface in ^{152}Sm from DPPQM

In the DPPQ model [7, 8], the potential energy function of the nucleus is given by Eq. (8)

$$V(\beta,\gamma) = \Sigma_{i\,\tau}\, v_i^2\eta_i - \Sigma_\tau\, g_\tau^{-1}\, \Delta_\tau^2 + (1/2)\, \chi^{-1}\beta^2. \qquad (8)$$

Here *i* represents all the deformed quasiparticle (dqp) states of the two oscillator shells, v_i^2 is the occupation probability of a dqp state, η_i is the dqp energy, g_τ is the pairing strength (τ = n, p) and Δ_τ are the calculated pairing gaps. In the last term, the coefficient $\chi = X \times A^{-1.4}$ (MeV) is the quadrupole force strength. Here we take X=70.0 (a regional value). Thus the PES V(β, γ) in DPPQ model takes into account the quasi-particle energies (along with occupation probabilities), the pairing gap and the quadratic deformation dependence.

The potential energy curve (PEC) V(β, γ=0^o) in ^{152}Sm from the DPPQ model is depicted in Fig**.** 3. The V_{min} lies on the prolate side at β=0.24, γ=0°, about 3.3 MeV below the spherical barrier at β=0. The horizontal line marked as 'ZPE' denotes the zero point energy and lies ~1.37 MeV below the spherical barrier. It signifies a spread from β=+0.11 to +0.41, representing softness in the β degree of freedom of the transitional nucleus at *N*=90. The oblate minimum lies at β = -0.11 and is only 0.80 MeV deep. The 0.685 MeV 0_2^+, 0.810 MeV 2_β and 1.085 MeV 2_γ levels lie within the prolate part of the PEC. Also the second excited 0_3^+ state at 1.082 MeV, lies below the spherical barrier. The 2^+ states have more than 92% main *K*-component in all the 4 bands. The nucleus can move from prolate to oblate side directly also. The higher bands $K^{\pi}=2_2^+$ and $K^{\pi}=4^+$, lie above the spherical barrier and oblate minimum, and hence exhibit mixing of prolate, oblate and spherical shapes, resulting in larger *K*-admixtures (Table II). The β_{min} of the

0_2^+ state will be slightly less than β_{min} for the ground state, but on account of the larger spread in quadrupole deformation β, its β_{rms} is predicted to be larger (Table II).

Jing-Ye Zhang *et al*. (1999) [18] deduced the PEC for ^{152}Sm, using the Generalized Collective model (GCM) [19], in a simplified form (comprising the β^2, β^4 and $\beta^3\cos3\gamma$ terms), and first term of the kinetic energy expression. This enabled them to reduce the 8 free parameters to three for PES (Fig. 5 in [18]). Their PEC is less deep, and the 'ZPE' lies just below the spherical barrier, so that only low spin states of ground band lie within the deformed prolate part, and 0_2^+ state lies above the spherical barrier, leading to smaller effective β. This contributes much greater spherical component in the calculated wave functions (Fig. 4 in [18]) for the β-band. Compared to PEC in [18] from GCM, in the DPPQM, no free parameters (except quadrupole strength *X*, regional value adopted) are used, nor the form of the potential is specified (see Eq. 8).

D. *B*(*E*2) values for g-,β- and γ-band

1. *Role of controlling parameter ε/k in IBM*

To resolve the shape co-existence anomalies (sec. IIIA), we performed the calculation in the 2-term IBM-1 Hamiltonian [9] (Eq. 6) for ^{152}Sm. We varied the quadrupole strength *k* (15 to 22.5 keV), and the boson energy ε (see Figs. 4 and 5), so as to reproduce the $E(2_g)$ energy. The plots of *B*(*E*2) values for β-g transitions, illustrated in Fig. 4, yield interesting features of the algebraic IBM. Firstly, $B(E2, 2_\beta \rightarrow 0_g)$ in IBM-1 (lowest curve in Fig. 2) is very weak (maximum value is 0.003 e^2b^2 compared to 0.005 e^2b^2 in experiment). The $(2_\beta \rightarrow 2_g)$ and $(2_\beta \rightarrow 4_g)$ curves also lie low. The increase of boson energy ε affects the prohibited β-g transitions only slightly, and they remain weak in IBM-1. The $B(E2, 0_\beta \rightarrow 2_g)$ value rises sharply with increasing value of ε/k, meeting the experimental value (0.16 e^2b^2 ~33 W.u) at ε/k =29. (The energy $E(0_2^+)$ also varies with ε/k). This transition is often used to test the collectivity of the 0_2^+ state. The anomaly of these two strong cross over *E*2 transitions (of 0_β-2_g,2_β-4_g) in experiment was noted in Ref. [12] (see below).

The plots of B(E2) values for transitions from 2_γ and 3_γ states are given in Fig. 5.

The lowest curve, of weak B(E2, $2_\gamma \rightarrow 0_\beta$), has a minimum at ε/k ~26, as also noted in [6] (on a log scale). The weak $B(E2, 3_\gamma \rightarrow 2_\beta)$~ (0.1 W.u or 0.0005(5) e^2b^2), also prefers ε/k=25-26. The $B(E2, 2_\gamma \rightarrow 0_g)$ and $B(E2, 2_\gamma \rightarrow 2_g)$ for γ-g transitions are almost constant,. But the $B(E2, 2_\gamma \rightarrow 2_\beta)$ =0.13 e^2b^2 prefers low ε/k, on the sharply falling curve. This illustrates the strong γ-β band mixing as predicted in the SU(3) symmetry of IBM.

The energy $E(2_g)$ =119 keV at ε/k =29, (k=17.5) is almost equal to experiment. For fixed k, it goes down with decreasing ε/k. though the energy ratio $R_{4/2}(=E_4/E_2)$ varies slowly from 3.0 to 3.09. If one prefers to reproduce the $E(2_g)$ value, which fixes the energy scale of the ground band, a value of ε/k =28 or 29 is preferable. After studying the variations in energy and $B(E2)$ values with the control parameter ε/k and for different k values, we have adopted the best fit value of ε/k =29 and k=17.5 keV. The partial level spectrum (limited to 4 bands) in IBM, compares well with data (Fig. 6), though the excited bands are somewhat expanded, as also in Ref. [12] for ε/k=30.

2. *Ground band*

The intraband $B(E2)$ values for the cascade $E2$ transitions in the ground band of ^{152}Sm are listed in Table III. In X(5) symmetry, Casten *et al*. [2] estimated the values normalized to $B(E2, 2_1^+\text{-}0_1^+)$ of 0.69 e^2b^2, which predict within (20 %) of the experiment. In a 2-term H_{IBM} with ε/k = 29.0, we have evaluated the ^{152}Sm spectrum (Fig. 6) and the B(E2) values (Table III). IBM values agree with experiment except at high spins. The DPPQ model values (up to I=6) are in good agreement with data.

TABLE III. $B(E2)$ values (e^2b^2) in the ground band. P=present. e_b=0.16, e_n=0.65.

I_i	I_f	E_γ keV	Expt.[4]	DPPQ	IBM[12]	X(5)[2]	IBM(P)
2_1^+	0_1^+	121.8	0.69 1	0.63[a]	0.69	0.69	0.69
4_1^+	2_1^+	244.7	1.00 2	0.95	1.02	1.09	1.015
6_1^+	4_1^+	340.4	1.17 2	1.12	1.12	1.36	1.117
8_1^+	6_1^+	420	1.366			1.566	1.141
10_1^+	8_1^+	483	1.53			1.80	1.10

a) Normalization will raise these values to 0.69, 1.00 and 1.17 e^2b^2 respectively.

3. K^{π}-0_2^+ β-*band*

The absolute B(E2) values for the transitions from the $K^{\pi}=0_2^+$ β-band are given in Table IV, along with the IBM-1 values, and the dynamic PPQ model values. We have taken the boson charge e_b of 0.16 and χ= -1.25 **(**rotor value**).** Our IBM-1 values are almost the same as in [12], except for $0_\beta \rightarrow 2_g$ and $2_\beta \rightarrow 4_g$, being smaller in both cases. The variation with ε/k in Fig. 4 does not account for this difference with [12]. The $B(E2, 4_\beta - 6_g)$ is anomalously high (factor of 10) in X(5), as also noticed in Ref. [2], and in IBM. In DPPQM (e_n=0.65) it is significantly closer to data, though still large.

In X(5) symmetry, which represents the transition to the deformed regime, the $B(E2, 2_\beta \rightarrow 0_\beta)$ and $B(E2, 4_\beta \rightarrow 2_\beta)$ *intraband* transition values, normalized to $B(E2, 2_g-0_g)$, agree with experiment. The ratio $B(E2, 2_\beta - 2_g/4_g)$=0.25 in X(5) compares well with 0.32(6),.and Alaga value of 0.55. Similarly, $B(E2, 2_\beta - 0_g/2_g)$= 0.22 in X(5), is close to 0.17(5), lower than the Alaga value of 0.7. Thus, the $B(E2)$ ratios for β-g are reproduced well in X(5) symmetry [1,2].

TABLE IV. Absolute $B(E2)$ (e^2b^2) ×100 values for $E2$ transitions in $K^{\pi}=0_2^+$ β-band at 684.8 keV in ^{152}Sm and B(E2) ratios. P=Present.

I_i	I_f	E_γ keV	Expt [4,12]	DPPQ	IBM[12]	X(5)[2]	IBM-P
0_β	2_g	563.0	15.7 11[a]	16.5	26	43[d]	16
2_β	0_g	810.5	0.5 1	0.22	0.05	1.4[d]	0.09
	2_g	688.7	2.6 3	2.9	4.8	6.2[d]	4.8
	4_g	444.0	9.2 9	8.9	9.5	25[d]	4.82
	0_β	125.6	53 5	65	43	54	43
4_β	2_β	212.4	102 3[b]	111	68	82	67
	2_g	901.2	0.33 8[b]	0.06	0.05	0.5	0.06
	4_g	656.5	2.6 6[b]	2.6	3.9	4.3	4.7
	6_g	316.1	1.9 9[b,c]	8.2		19[d]	23
6_β	$4_\beta/4_g$	288/944	59 3	13×10^4			1.0×10^3
	$4_g/6_g$	944/603	0.65 5	0.04×10^{-2}			0.02

a) Casten *et al*. [6]. b) Klug *et al.* [20]. c) Reduced from 3.0 in [4].
d) The large deviations in X(5) for these interband transitions are reduced, by using the deformation dependent inertia tensor (see Ref. [21]).

The large intraband value of $B(E2, 2_\beta \rightarrow 0_\beta)$ (111 W.u [12, 20]), almost equals $B(E2, 2_g \rightarrow 0_g)$=144, a rotational model value, as well as $\Delta E(2_\beta\text{-}0_\beta)$ of 126 keV, nearly the same as the 2_g value, signify the presence of rotor model features in the β-band of ^{152}Sm. This is given well in IBM. Similarly, the large $B(E2, 4_\beta \rightarrow 2_\beta)$ =1.57 e^2b^2~ 330 W.u [12], revised to ~1.02e^2b^2 by Klug *et al*. [20] from life time measurement, is supported in IBM. The large interband $B(E2, 0_\beta \rightarrow 2_g)$ = 0.16 e^2b^2~33 W.u [4,12] (unexpected in 2-state band mixing method of BM model}, is reproduced in the DPPQM and our IBM-1 calculation (see Fig. 4 and role of the control parameter). No charge adjustment of the *E*2 operator is done here in DPPQM. The IBM-1 interband values for $B(E2, 2_\beta \rightarrow 0_g)$ and $B(E2, 4_\beta \rightarrow 2_g)$ are significantly lower than experiment, a usual feature in IBM. Zamfir *et al*. [12] noted the two strong cross over transitions to the deformed yrast band (0_β-2_g of 33 W.u. and 2_β to 4_g=19 W.u) in experiment, seem to be inconsistent with the (assumed) spherical 0_2^+ and 2_β states, along with other inconsistencies in this extreme proposition [12].

.Zamfir *et al*. [12] discussed the anomalies of the 2-state band mixings in rotor model framework for β-g transitions. As cited in the introduction, 2-state mixings failed to obtain consistent Z_β in shape transitional nuclei [5]. However, in the DPPQ model, wherein full band mixing is allowed, both intraband and interband *B*(*E*2) values are consistent with data simultaneously (see [8] for earlier studies in DPPQM, before the advent of IBM).

In a recent review of the problem of the global validity of the axially symmetric vibration view of β-band, Gupta and Hamilton (2015) [22] presented evidence in its support for the A=140-180 region of the nuclear chart. It was also pointed out therein that the weak β-g transitions arise also on account of the formation of a node in the wave function of 0_β state, as illustrated here for ^{152}Sm (Fig. 7), resulting in poor overlap with ground band wave functions.

In Ref. [22] we noted that $B(E2, 0_2^+ \text{-} 2_g)$ is large (0.26 e^2b^2) at *N*=88 in ^{150}Sm which drops to 0.16 (1) in ^{152}Sm, further reducing to only 0.06 in ^{154}Sm. In Gd isotopes this feature is further highlighted [22]. This trend was reproduced in DPPQM (see Table I and Fig. 13 in [22]). The *role of β-softness versus β-deformation is apparent* here. The node for 0_β {Fig. 7) also signifies β-softness. Lowering of the 0_2^+ state (falling even

below 4_g in ^{152}Gd) at N=88, explains these features. The competition between the quadrupole interaction and the pairing interaction leads to these special features as illustrated for ^{150}Sm in Ref. [23], where the role of the control parameter ε/k in IBM-1 was also illustrated. These features fully support the axially symmetric β-vibration view in ^{152}Sm (and other N=90 isotones), and the shape coexistence view does not hold here.

4. $K^\pi=2^+$ γ-*band*

The absolute $B(E2)$ values for intraband transitions in the K=2 γ-band and for interband γ-g and γ-β transitions from Ref. [4, 6, 12] are listed in Table V. The small value of B(E2, $2_\gamma \rightarrow 0_\beta$) of 0.0008 e^2b^2 (<0.05 W.u) [12], is well reproduced in the DPPQ model and reasonably in X(5) (larger in IBM for ε/k =28-30). The small value of R^{γ}_{0g}= $B(E2;2_\gamma \rightarrow 0_\beta)/B(E2;2_\gamma \rightarrow 0_g)$ = 0.048(4), which led to the proposition of the shape coexistence, is also indicated (=0.022) in DPPQ model. Also the large B(E2, $2_\gamma \rightarrow 2_\beta$)=0.13(2) e^2b^2 [5] is reproduced in DPPQM. In the 2-parameter IBM-1, the value of 0.13 corresponds to a low value of ε/k. Most values for 4_γ also are given fairly well in DPPQM and IBM (within a factor of 2 or 3). The X(5) values, normalized to $B(E2;2_\gamma \rightarrow 0_g)$ are in accord with experiment.

TABLE V. Absolute B(E2) values (e^2b^2)×100 for $E2$ transitions in $K^\pi=2_1^+$ γ-band at 1085.8 keV in ^{152}Sm. ε/k =29 for IBM(P) and =30 for IBM [12].

I_i	I_f	E_γ keV	Expt.[4]	DPPQ	IBM[12]	X(5)	IBM-P
2_γ	0_g	1085.8	1.7 1	2.3	1.4[c]	1.7[g]	3.5
1086	2_g	964.1	4.5 3	4.9	1.4[c]	2.5	5.5
	4_g	719.3	0.5 1	0.57	1.9	0.13	2.1
	0_β	401.3	<0.08[a]	0.05	1.0	0.15	0.70
	2_β	275.4	13 2[b]	12	44[d]		42
4_γ	2_g	1249.9	0.24	0.9			1.03
1371	4_g	1005.3	2.7 8	4.8			4.7
	2_β	561.3	0.12	0.16			0.61
	4_β	349.8	<17	5	12		9
	2_γ	285.8	25	36	30		34
	3_γ	138	<125	71			45
3_γ	2_β	423.5	0.10[e]	0.10		0.20	2.06[f]
1234	2_γ	148		95		84	79

a) Ref. [6]. b) Listed as M1 in [3]. c) Seem misprinted in [12].
d) See the sharp rise of the curve in Fig.5, to yield large value in IBM.
e) Ref. [24].
f) See the sharp rise of $B(E2, 3_\gamma \rightarrow 2_\beta)$ curve at $\varepsilon/k \geq 28$ in Fig.5.
g) Normalized to $B(E2, 2_\gamma \rightarrow 0_g)$ in experiment [25].

Zamfir *et al*. [24] re-measured the lifetime of the 3_γ state in ^{152}Sm, using the γ-ray induced Doppler technique in the (n,γ) capture reaction, and deduced the $E2/M1$ mixing ratio of the $3_\gamma \rightarrow 2_\beta$ transition from linear polarization measurements of γ-rays following the ε decay of ^{152}Eu. We reproduce the same in DPPQ model (Table V). In IBM for ε/k=28-30, it exceeds the datum (see the curve in Fig. 5). The $B(E2)$ ratios for $E2$ transitions (derived from E_γ and I_γ) from 3_γ to g- and β-band (Table VI) are fairly reproduced in DPPQM (within a factor of 2), better than in IBM. Same is true for transitions from 5_γ and 6_γ states

These facts related to IBM and X(5) signify an important systematic trend, that the intrinsic structure of β- and γ-band corresponds to deformed or SU(3), but the interband $E2$ transitions require higher ε/k for β-band and lower for γ-band.

TABLE VI. $B(E2)$ ratios in $K^\pi=2^+$ γ-g transitions. Energy levels and E_γ are in (keV).

I_i I_f/I_f'	$E_\gamma/E\gamma$' [3]	I_γ/I_γ [3]	Expt.	DPPQ	IBM-P
3_γ1234					
$2_g/4_g$	1112.1/867.4	100/30.9	0.93 1	1.3	0.89
$2_\beta/2_g$	423.5/1112.1	0.022/100	0.027 4	0.055	0.36[a]
$2_\gamma/2_g$	148/1112.1	0.15/100	36 4	25	14
$4_\beta/2_\beta$	211/423.5	0.028/0.022	42 5	36	9[a]
5_γ1559					
$4_g/6_g$	1193.1/852.7	100/38.1	0.49 3	0.76	0.58
$3_\gamma/4_g$	325.7/1193.1	4.7/100	31 3	22	16
6_γ 1728					
$4_g/6_g$	1362/1021.4	20.6/100	0.05 1	0.09	0.13

a) See Fig. 5 indicating the sharp rise of B(E2, $3_\gamma \rightarrow 2_\beta$) curve at ε/k=28-30

E. $B(E2)$ ratios from $K^+=0_3^+$ band, 0_4^+ state and $K^\pi=2_2^+$ band

1. *Second excited 0_3^+ band*

The contribution of single particle aspects may become important at higher energies, for example, in 0_3 and 0_4 bands. However, the collective models can indicate how far the collective models work. If the collectivity as indicated in the intraband B(E2)s and reflected in the ratios is substantial, the nomenclature of multi-phonon bands may be used in favorable cases as in the N=90 soft rotors. The multi-phonon term need not imply harmonic vibrations. In general it remains an open problem.

The ratio $B(E2, 0_3^+ - 2_\beta/2_g)$ of >40 [3,4] in experiment, is 126 (3-times larger) in DPPQM (Table VII). It is >350 in IBM, too large, because the $B(E2, 0_3^+ \rightarrow 2_\beta)$ is large by a factor of three, and $B(E2, 0_3^+ \rightarrow 2_g)$ =0.001.is too small compared to ~0.005 e^2b^2 [20] in experiment. The $B(E2, 2_{03}^+ - 2_\beta/2_g)$ ratio of ~ 16 in IBM is far from 56(5). Similarly, $B(E2, 2_{03}^+ - 0_3^+/0_\beta)$ is too small in IBM. For a better comparison of large value in experiment and DPPQM, the 10^2 factor is used here.

TABLE VII. $B(E2)$ ratios from 1082.8 keV 0_3^+, 1292.8 keV 2_4^+, 1612 keV 4^+ and 2004 keV 6^+ states.

I_i I_f/I_f'	$E_\gamma/E\gamma$' [3]	I_γ/I_γ [3]	Expt. [3]	DPPQ	IBM-P
$0_3^+ - 2_\beta/2_g$	272.4/961.1	7.8/100	43 6[a]	126	368
$2_{03}^+ - 0_3^+/0_\beta$	210/608.1	1.58/0.1	32 15 $\times 10^2$	25 $\times 10^2$	19
$0_g/4_g$	1292.8/926.3	37/100	0.07 1	0.26	9
$2_\beta/2_g$	482.4/1171	9.1/13.7	56 5	80	15.5
$0_\beta/0_g$	608.1/1292.7	0.1/37	0.12 4	0.12	6.8
$2_\gamma/2_\beta$	207/482.4	0.42/9.1	3.2 8	3.6	1.1
$4_{03}^+ - 2_{03}/2_\beta$	320.1/802	21.4/4.5	470 70	220	
$2_\beta/2_\gamma$	802/527.2	>4.5/2.0	>0.28 3	6.3	
$2_\beta/2_g$	802/1491.4	4.5/6	17 10	1.5	
$4_\beta/4_\gamma$	589.8/241.7	14.2/4.1	>0.04	106	
$4_\beta/4_g$	589.8/1246.2	14.2/10.1	59 12	76	
$4_g/6_g$	1246.2/906.1	10.1/100	0.020 3	0.097	
$6_{03}^+ - 4_{03}/4_g$	391.3/1637.4	58.8/100	754 60	251	

a) Value reduced to 22 in [20].

In DPPQ model a 92% K=0 component is predicted for the $I^\pi=2_4^+$ state, associated with the 1292.8 keV level. The 1292.8 keV 2_{03}^+ level is 210 keV above the

1082.8 keV 0_3^+ level, larger than $\Delta\beta$=126 keV and 2_g=122 keV. But the large $B(E2, 2_{03} - 0_3^+/0_\beta)$=3(1)×$10^3$, (reproduced in DPPQM) indicates strong intra band relation (Table VII). The $B(E2, 2_{03}^+-2_\beta/2_g)$ =56(5), larger in DPPQM, supports its collective character. $B(E2, 2_{03}-2_\beta)$ = 0.07 e^2b^2 (~14 W.u) in DPPQM (same in IBM), favors mixing with β-band. Over all, there is fair reproduction of all the six interband $B(E2)$ ratios listed here, in DPPQM (Table VII).

The 1612.9 keV 4^+ state [3] decays to ground, β, γ and 2_{03}^+ states and thus may be the 4^+ member of the $K^\pi=0_3^+$ band head (not listed in [13]). The deduced $B(E2)$ ratios are listed in Table VII. The large $2_{03}/2_\beta$ $B(E2)$ ratio supports the band relation (DPPQM value is about half). The transitions to the γ-band stronger than to β-band are indicated. But in DPPQM the opposite trend is obtained, which is more probable for a $K^\pi=0_3^+$ to $K^\pi=0_2^+$ band transition. The transitions to g-band are weaker. The large B(E2) ratio of intraband transition from 6_{03}^+ (2004 keV) state to $4_{03}^+/4_g$ is also given well in DPPQM. Thus the $B(E2)$ ratio data for the band built on 0_3^+ state are fairly reproduced in the dynamic PPQ model to support its collective character.

The 2n transfer amplitude σ(t,p) and σ(p,t) provide important information on the nature of the excited states. McLatchie *et al*. (1969) [26] studied the 2n transfer cross section σ in ^{154}Sm(p, t)^{152}Sm reaction to identify the 0^+, 2^+ states in ^{152}Sm, and noted the 30% σ(p,t) for the 685 keV 0_β state and the vanishing σ(p, t) for the second excited 0^+ state at 1082 keV. Including the 2n transfer (t, p) results of Hinds *et al*. [17], they interpreted these results to suggest the spherical status of the 1082 keV 0_3^+ state. Debenham and Hintz (1972) [27] in the study of 2n transfer (p, t) suggested that the 0_3^+ state in ^{150}Sm is favored to be deformed as the g.s of ^{152}Sm. On the other hand, Borner *et al*. (2006) [28] in their study of ^{150}Sm suggested it to be an anharmonic vibrator. This view is in fact cited by Kulp *et al.* [13] for calling 0_3^+ as a "*pairing isomer*". Gupta *et al*. (2010) [23] illustrated the *soft rotor* characteristics in the excited 0^+ bands of ^{150}Sm. Using intrinsic state formalism [29] with parameters of H_{IBM}, the PEC for ^{150}Sm yielded finite deformation β >0, further confirming it as a soft rotor.

Earlier, the large 2n transfer cross section σ(t, p) in N=90 isotones (product) and σ(p,t) for N=88 (product) isotones for the excited states (cumulatively), relative to ground

state, were reproduced in microscopic treatment based on Nilsson orbits in Ref. [30] in (1995). Same were observed at *N*=98 and 108. The increased cross section was attributed to the shape change.

Fossion *et al*. [31] explained the peaks in (t, p) 2n transfer cross sections in *N*=90 Sm, Gd and other isotones, and correlated them with the shape phase transition on the U(5) to SU(3) path. They obtained enhanced σ for the excited 0_2^+ state in ^{150}Sm(t, p)^{152}Sm reaction using the s^+ boson number raising operator of IBM.

More recently, Zhang and Iachello [32] extended the work of Fossion *et al.* [31], and used IBM to derive 2n transfer amplitudes in Sm isotopes and showed that the large amplitudes indicate quantum phase transitions at *N*=88-90. Earlier, Clark *et al*. [33] reviewed the role of the 2n transfer reaction strength for the ground state and excited 0^+ states in deformed nuclei, vis-a-vis the shape co-existence view and the shape difference of the target and product nucleus. By comparing with the IBM predictions, they concluded that large σs (2n transfer) for (t, p) and (p, t) reactions arise from the shape difference. Thus we conclude that the pairing isomer view of 0_3^+ state is not valid here.

2. 0_4^+ state and $K^\pi=2_2^+$ band

TABLE VIII. *B*(*E*2) ratios for interband transitions from the 1658.8 keV 0_4^+, and 1769 keV 2_5^+ $K^\pi=2^+$ state. CE=Coulomb excitation

I_i I_f/I_f'	$E_\gamma/E\gamma$' keV	I_γ/I_γ [3]	Expt.	CE[13]	DPPQ
1658.8 keV					
0_4^+ $2_\beta/2_g$	847.5/1535.3	2.4/1.2	22 15		19
1769 keV					
$2_{\beta\gamma}^+$ $2_\beta/2_g$	958.6/1647.4	100/37	41 4	36	21
$2_\gamma/2_\beta$	683.2/958.6	24.1/100	1.3 1		0.64
$3_\gamma/2_\gamma$	535.4/683.2	8.8/24.1	1.2 1		7.2
$0_\beta/2_\beta$	1084/958.6	54/100	0.29 4	0.37	0.64
$0_\beta/0_g$	1084/1769	54/47.3	13 1	16	6400
$0_3/0_\beta$	476/1084	8.6/54	8.5		3.2
$4_\beta/2_\beta$	746/958.6			<0.012	0.01
1907.7 3^+					
$2_\beta/2_g$	1097/1786	98/100	11 2		19
$4_\beta/4_g$	884.8/1541	21.6/60	6 1		110
$2_\gamma/2_\beta$	821/1097	22/98	1.0 2		0.1

The increase of B(E2, $0_g \rightarrow 2_g$) with increasing Z, along with the increasing $E(2_{g,})$, in N=88 isotones, led to a breakdown of the Grodzins constant product rule [34], a surprising but a revealing fact, noted in Ref. [35] which again proved the importance of the softness of the nuclear core.

A 0_4^+ state at 1658.8 keV and a 1769 keV 2^+ state are listed in NDS [4]. These levels are also confirmed in the (n, n'γ) excitation functions of Ref. [13]. From the life time data, Kulp *et al*.[13] estimated B(E2, $0_4^+ \rightarrow 2_\beta$) =5(1) W.u. The DPPQM value (0.5 W.u) is 10 times weaker. But the B(E2, 0_4^+-$2_\beta/2_g$) ratio (Table VIII) is given correctly. Stronger decay 573 keV to 1086 keV 2_γ and 366 keV to 1293 keV 2_{03}^+ state are predicted in DPPQM, but not confirmed in experiment.

The fifth 2^+ state in DPPQM indicates 90% predominant K=2 character. Using the E_γ, I_γ values from nndc compilation (Table VIII), we have deduced the relative B(E2) ratios from the 1769 keV 2^+ state. The $B(E2)$ ratios from DPPQM agree reasonably well with data, except for the transition involving the decay to the 0_g state, for which the DPPQM value of 2×10^{-6} e^2b^2 is rather too low The decay to the 2_β, 2_γ and 3_γ support its βγ character.

Kulp *et al*. [13] from multi-Coulex experiment and the large array of Ge detectors determined the $B(E2)$ values for $E2$ transitions from the 1769 keV 2^+ state to the 0_2^+ β-band and ground band, and by comparison with Alaga values in the rotor model, assigned it to the $K^\pi=2^+$ βγ-band. The absolute $B(E2, 2_5 \rightarrow 2_\beta)$ =0.125 e^2b^2 (25 W.u) [13] exceeds the DPPQ model value of 0.025 by factor of 5. However, their deduced $B(E2)$ ratios are reproduced fairly well in DPPQM (column 5 in Table VIII).

The second $I^\pi=3^+$ state at 1907.7 keV decays to β-, γ- and g-band. The deduced $B(E2)$ ratios E_γ, I_γ values from nndc compilation [3] are exhibited in Table VIII. While stronger decays to β-band (2^+, 4^+) are supported in DPPQM, the equally strong decay to K=2 γ-band is not reproduced in DPPQM. With ~138 keV above the 2^+ 1769 keV state, it is a good candidate for the βγ-band, and supports the collective character of the band.

F. $K^\pi=4^+$ γγ band

The I=4 level at 1757 keV is the band head of $K^{\pi}=4^{+}$ band, with levels up to I=11, identified. The 1757 keV state de-excites to 2_{γ}, 3_{γ}, 2_{β}, 4_{β} and to ground band (I=2, 4). Using the E_{γ} and I_{γ} values from nndc [3], we have deduced the $B(E2)$ ratios. For the fifth 4^{+} state, DPPQM predicts 68% K=4 and 25% K=2 admixture which supports its K=4 predominant character. The values for $B(E2)$ ratios from the DPPQ model are given in Table IX. The basic pattern of decay, viz. stronger decay to $K^{\pi}=2^{+}$ γ-band, weaker to $K^{\beta}=0_2^{+}$ β-band and weak to ground band are predicted. In DPPQM, $B(E2, 4_{K=4}\rightarrow 2_{\gamma})$ = 0.043 e^2b^2 compared to B(E2, 2_{γ}-0_g) = 0.023 e^2b^2, indicates good band mixing with K=2 band The $B(E2, 4_{K=4}\rightarrow$β-band) is slightly larger (than expected) in DPPQM, which renders the related $B(E2)$ ratios smaller than experiment (Table IX). But the $B(E2, 4_{\gamma\gamma}\rightarrow 3_{\gamma}/2_{\gamma})$ and $B(E2, 4_{\gamma\gamma}\rightarrow 4_{\gamma}/2_{\gamma})$ are fairly well predicted.

The basic trend of decays from $5_{K=4}$ state also is given fairly well (within 2σ deviations) in DPPQM (Table IX), supporting the K=4 γγ assignment. Intra band transitions from 2040 keV $6_{\gamma\gamma}$ to $4_{\gamma\gamma}$ and $5_{\gamma\gamma}$ states are also strong (Table X). Energy levcls up to spin $I^{\pi}=11^{+}$ in the $K^{\pi}=4^{+}$ are identified for this band. $E2$ transitions from higher spin states to K=2 and K=4 states are given without I_{γ} values in the nndc compilation [3]. However, even the partial data support the band formation.

TABLE IX. $B(E2)$ ratios for interband transitions from the $K^{\pi}=4^{+}$ band at 1757 keV.

I_i $I_f/I_{f'}$	$E_{\gamma}/E\gamma'$ keV	I_{γ}/I_{γ} [3]	Expt.	DPPQ
1757 keV				
$4_{\gamma\gamma}$ $3_{\gamma}/2_{\gamma}$	523.1/671.1	62.5/100	2.2 5	1.7
$4_{\gamma}/2_{\gamma}$	385.6/671.1	22.7/100	3.6 8	1.2
$2_{\beta}/2_g$	946.5/1635.4	4.5/0.66	105 40	204
$4_{\beta}/4_g$	734.1/1390.5	3.7/17.4	5.2 11	31
$2_{\gamma}/2_{\beta}$	671.1/946.6	100/4.5	124 41	6.2
5^{+} 1891				
$3_{\gamma}/4_{\gamma}$	657.4/519.9	85/100	0.26 4	0.36
$5_{\gamma}/4_{\gamma}$	331.5/519.9	65/100	6 2	1.3
$4_{\gamma\gamma}/4_{\gamma}$	134.7/518.9	56/100	475 110	19

TABLE X. $B(E2)$ ratios for interband transitions from $K^{\pi} = 4^{+}$ band with level energies of (2040, 2208, 2391, 2588, 2810 and 3017 keV) for I=6^{+} to 11^{+}.

I_i $I_f/I_{f'}$	$E_\gamma/E\gamma'$ keV	I_γ/I_γ [3]	Expt.	DPPQ
2040 keV				
6^{+} $4_{\gamma\gamma}/6_g$	284/1333.3	27/100	$6(1) \times 10^2$	b)
$5_{\gamma\gamma}/6_g$	149/1333.2	41/100	$23(4) \times 10^3$	
$7_{\gamma\gamma}$ $6_\gamma 6_g$	478/1499	a)		
8_γ-$8_\gamma/8_g$	727/1267	a)		
$9_{\gamma\gamma}$-$8_\gamma/8_g$	195/1463	a)		
$10_{\gamma\gamma}$ -10_γ	730	a)		
$11_{\gamma\gamma}$- $9_{\gamma\gamma}$	440	a)		

a) No I_γ listed in [3]. b) not calculated.

The $K^{\pi}=4^{+}$ $\gamma\gamma$ band assignment is well supported in our calculation, though a small $E4$ component admixture 0^{+} ground state to 4_{K-4} (corresponding to 6% K=0 component) is possible. The energy ratio R=E($4_{K=4}$)/E(2_γ) =1.62 indicates large anharmonicity. This is different from the anharmonicity in well deformed nuclei (e.g. R>2.0 for ^{168}Er), due to the simultaneous β-softness as well. The γ_{rms} =25° for this band (22.5° for K=2 γ-band) for the axially symmetric deformed nucleus of ^{152}Sm, indicates large softness to γ-vibration and γγ-vibration (see the PEC curve in Fig. 3). The odd-even spin staggering in the K=4 band here, also indicates large γ-softness.

IV. EMPIRICAL FEATURES

A. Deformation and softness of β-band

The empirical analysis of the energy level structure of a band provides subsidiary information, on its deformation status. The level energies in the ground band of an even Z even N nucleus can be expressed by a single term formula, called the power index formula [36]

$$E(I) = a\, I^{b}. \qquad (9)$$

Here, the power index 'b' may vary between 1.0 and 2.0. The scaling coefficient 'a' corresponds to the inverse of the moment of inertia. Validity of the formula, in

reproducing the level energies from the average values of '*b*' and '*a*' for up to $I^{\pi}=12^{+}$ has been well illustrated in Refs. [36,37]. For ^{152}Sm ground state band, the energy level spectrum calculated by the power index formula illustrated in Fig. 8 exhibits its validity.

The formula also works well for the $K^{\pi}=0_2^{+}$ band by writing

$$E(I) = E0 + a\, I^{b} \qquad (10)$$

Here *E0* is the band head energy. The values of power index '*b*' for the ground band and the β-band of ^{152}Sm are illustrated in Fig. 9.

Firstly, from the figure one can see that the power index '*b*' (~1.50) for the β-band is lower than ~1.60 for the ground band (for deformed ^{154}Sm, '*b*' ~1.70). This is the effect of the lower $R_{4/2}$ value of 2.69 for the β-band compared to 3.01 for the ground band. Secondly, in β-band, the index value is lower at spin *I*=4, than for the rest of the band, and there is less constancy with spin. In view of the fact that the 2^{+}-0^{+} energy difference in the β-band is almost the same as for ground band, it is apparent that the smaller *E*(4)-*E*(2) interval in the beta band is the source of the anomalous $R_{4/2}$ value in ^{152}Sm. At higher spin, the β-band is more rotational. The figure also illustrates the repeating structures of the two bands. These features of β-band are also reflected in ^{154}Gd (Fig. 9) and ^{156}Dy (not shown). It is apparent that the assumption of spherical status for $K^{\pi}=0^{+}$ β-and is an extreme proposition.

B, Odd-even spin Staggering in γ-band

The well known odd-even spin staggering in $K^{\pi}=2^{+}$ γ-bands, as expressed by the staggering index S(4), provides a useful test of the deformation status of the band. In a previous study of the systematics of the γ-bands in rare earth region in Ref. [38], it was demonstrated that S(4) falls with increasing deformation of the band. Casten *et al*. [39] suggested the formula for S(I):

$$S(I) = R(I)/R(I)_{adiabatic} - 1, \qquad (8)$$

where $R(I) = 2(E_I - E_{I-1})/(E_I - E_{I-2})$. S(I) is zero for good rotor (adiabatic) and is (-1) for degenerate (4_γ, 3_γ) in harmonic vibrator. The plots of S(I) for Sm, Gd and Dy for *N*=88-

92 are displayed in Fig. 10. The value of |S(4)| is large at N=88 (~0.5), and drops sharply at N=90 (~0.15), and further at N=92 (<0.05) in Sm, Gd and Dy. Also, the quadrupole moment ratio Q_{22}/Q_{00}=1.0(1) also supports the deformation of 2_γ state [40]. Thus, the γ-band staggering in N=90 ^{152}Sm favors its near deformed character. This is an additional, model independent, evidence against the shape coexistence (n=2 spherical phonon triplet on 0_2^+) proposition cited above.

V. **DISCUSSION AND SUMMARY**

A. Discussion

(i) The important issue of current interest is the proposition of *shape coexistence* of the assumed 2-phonon triplet based on 0_2^+ state with 2_2^{+-} as 1-phonon state in ^{152}Sm. The irrefutable facts are: $R_{4/2}$ for ground band is 3.01 and $R_{4/2}$(4-2)/(2-0) is 2.69 for β-band. $E(2_\beta)$-$E0_\beta$) = $E(2_g)$. The energy $E(0_2^+)$ is very low and 2_β lies below 2_γ. Almost constant power index 'b' for ground band and β-band Eqs. (9 and 10) (Fig. 9) reflect the uniform structures of these bands. The odd-even spin staggering in γ-band (Fig. 10) shows its almost deformed status. Intraband B(E2) transitions in β-band are almost as strong as in the ground band. Cross over β-g interband transitions are collective. All these features, reflecting the shape transitional nucleus ^{152}Sm, display the collective quadrupole character of the β- and γ-bands. The assumption of the deformed ground band and spherical 0_2^+ is an extreme proposition. The supporting features for the latter include weak (vanishing) B(E2, 2_γ-0_β), weak B(E2, 3_γ-2_β), value, weak B(E2, 2_β-0_g) and B(E2, 2_β-2_g). It should be noted that the former two transitions are cross over transitions (Fig. 1), hence weak . The IBM under-predicts, or predicts for specific values of the controlling parameter ε/k [6,12], the latter features. However, these are well reproduced in DPPQM.

(ii) In IBM-1 framework, Zamfir *et al*. [12] studied the distribution of n_d bosons in the states of β-band and noted the predominance of n_d =0-1 bosons, different from the pattern for the ground state, which supports the shape coexistence view. From a comparison of different dependence of $B(E2)$ in β-, and γ-bands on ε/k control parameter (Figs. 4, 5) and the role of kinetic coefficients in DPPQM, it is indicated that besides the

nuclear shape, the softness (fluctuations) of the nuclear core plays a major role here in the N=90 shape transitional nucleus ^{152}Sm.

(iii) Jolie *et al*. [41] gave a different view on the shape coexistence proposition. Burke [42] analyzed the reasoning cited in [6, 11, 12], based mainly on the weak γ-β $E2$ transition in ^{152}Sm, and pointed out the inconsistency in assuming the shape co-existence. Later, Clark *et al*. (2003) [33], using band mixing and the results of DPPQM [8] for ^{152}Sm, obtained results in agreement with experiment and found no compelling need of the proposition of shape co-existence in ^{150}Nd and ^{152}Sm.

(iv) It may be of interest to note that in the spherical ^{150}Sm nucleus too, the B(E2) values in interband and intraband transitions exhibit quadrupole deformation effects [22,23]. The *anomaly of shape coexistence gets resolved* if one notes that the shape transitional nucleus ^{152}Sm (and other N=90 isotones), lie at the shoulder of the spherical to deformed transition path. So the features of both spherical and deformed are simultaneously present in these nuclei in the ground band and as well as in beta band, (as also in N=88 nuclei), exhibited in different physical entities. The very low energy of 0_β in N=88 and N=90 isotones signifies the highly β-soft nature of the β-band. As stated above, the fluctuations in the β, γ degrees of freedom, affect the $E2$ transition rates and the variations in the kinetic coefficient $B_{\beta\beta}$ adds to the dynamics.

(v) Earlier, Kumar (1974) [8] explained the large cross section σ(t, p) for 2n transfer for the excited 0^+ states [17], without assuming a spherical shape of 0_β band and 0_3^+ band in ^{152}Sm and suggested that this weak evidence may not be decisive. Kumar [8] questioned this interpretation on the grounds that one does not get two potential energy curves (PEC) minima in either of the nuclei. Further, according to the recent findings by Clark *et al*. (2009) [43], it is explained that a large 2n(t, p) and 2n(p, t) cross section of an excited 0^+ state [17] arises due to shape difference between the target and product nucleus, in agreement with the findings of Ref. [8]. Zhang and Iachello [32] illustrated the quantum phase transition at N=88=90 through the reproduction in IBM of the large amplitude of σ(t, p) and σ(p, t) reactions. According to DPPQ model almost the same deformation is obtained for the three K-bands in ^{152}Sm [8]..

(vi) It is well known that the SU(3) symmetry corresponds to axially symmetric deformed rotor symmetry, but there are *distinct differences* too. Earlier, at the advent of IBM and its

dynamical symmetries, Gupta (1986) [44] discussed the problems of identifying possible candidates for the pure SU(3) symmetry limit. An obvious, well known example, are the γ-g, and β-g (2^+-0_1^+) *E*2 transitions, *allowed* in BM unified collective model (Alaga rules), but *prohibited* in the pure SU(3) limit of IBM, and needing different symmetry breaking to induce the γ-g and β-g transition in deformed rotor nuclei. In Ref. [44], the features of SU(3) symmetry vis-à-vis β, γ-bands and the ground band were illustrated in detail. Only the O(3) symmetry is well related systematically to the N_pN_n product.

Arima and Iachello [45] noted the formal identity of the SU(3) symmetry applied by Elliot [46] to the sd shell, and the differences too, since the former applies to bosons and the latter to fermions. For higher Nilsson shells, the long range separable Q·Q interaction restores the SU(3) symmetry, broken by the intruder orbit $\pi(h_{11/2})$ for this region, and produces the deformation of the rotor model.

B. Summary

The long history of the controversy regarding the spherical shape of the $K^\pi=0_2^+$ β-band along with the soft deformed ground band of the transitional nucleus ^{152}Sm and other *N*=90 isotones is reviewed here. The slight difference in deformation in the two bands is well visible (Fig. 9), but the level patterns can be viewed in both ways, viz. the anharmonic vibrator view and the *K*-band view (Fig. 1). The illustrations (Figs. 4 and 5) of the dependence of β-g, γ-g and γ-β *E*2 transition strength on the SU(3) symmetry breaking term as expressed by the controlling parameter ε/k in IBM-1 framework reveals the power of IBM and its limitations vis-à-vis more microscopic theories. The problem of the choice of freely adjustable H_{IBM} parameters for transition between the limiting symmetries U(5) and SU(3) is illustrated through the analysis of Figs. 4 and 5. While the energy scale and the β-g transitions favor larger SU(3) symmetry breaking (more vibrational), the γ-g and γ-β transitions favor lower ε/k value.

However, the intra band *B*(*E*2) values clearly favor the rotational features in the β-band and the other excited bands as well. The predictions of the dynamic PPQ model, viz. *K*-admixtures, β_{rms}, γ_{rms}, absolute *B*(*E*2) values for intra band transitions and interband transitions, all agree fairly well with experiment, as also demonstrated in the

early work of Kumar [8]. But the level energy predictions for higher lying bands remains poor and set a limitation on its full capacity, though the level patterns are well given.

The ratio $B(E2, 0_3^+ - 2_\beta/2_g)$ of >40 [3,4] in experiment, and supported in theory, supports it as 2β-phonon character. The intra band transitions in the $K^\pi=0_3^+$ band from the 2_{03}^+ and 4_{03}^+, fairly reproduced in DPPQM, also support the 2β character.

Here the subtle difference between the shape coexistence leading to "pairing isomer" interpretation of the 2n transfer data, and the shape transition at *N*=88-90, as prevalent in literature for the last five decades is reviewed. The collectivity of the 0_3^+ band as expressed in intraband and inter band transitions is illustrated. The subtle difference between the SU(3) symmetry in IBM frame work and the Rotor model features in the shape transitional nucleus is pointed out. Also the different roles of level energies in the *N*=88, 90 isotones and the *B*(*E*2) values, as high lighted in the deviations from the Grodzin's product rule, yield new insights into the complex interesting structure of these low 0_2^+ nuclei. It also demonstrates the charge dependence of the nuclear force for the strength of the electro magnetic interactions.

The multiphonon nature of the $K^\pi= 2_2^+$ βγ-band and $K^\pi= 4^+$ γγ-band in ^{152}Sm is supported. We have also pointed out that the shape co-existence is not controversial. Rather the β-band in ^{152}Sm exhibits mixed features of the rotation and vibration, it being a nucleus at the border line of the two types of motion, which are not exclusive. Here one has to take into account the shape of the higher bands as well. The ^{154}Gd and ^{156}Dy *N*=90 isotones have similar band structures, and the seven *K*-bands in ^{154}Gd have been studied in DPPQM [47], which supports the formation of similar *K*-bands in the *N*=90 isotones.

ACKNOWLEDGEMENT

J. B. Gupta appreciates the post retirement association with Ramjas College, University of Delhi. The work at Vanderbilt University is supported by the U.S. Department of Energy under Grant No.DE-FG02-88ER40407.

RERFERENCES

[1] F. Iachello, Phys. Rev. Lett. **87**, 05-2502 (2001).

[2] R.F. Casten and N.V. Zamfir, Phys. Rev. Lett. **87**, 05-2503 (2001).

[3] Brookhaven National Laboratory, Chart of nuclides of National Nuclear Data Center, http:\\www.nndc.bnl.gov/ENSDF.

[4] M.J. Martin, Nuclear Data Sheets **114**, 1497 (2013).

[5] J.H. Hamilton, F.E. Coffman, A.V. Ramayya and K. Baker, Phys. Rev. **C3**, 960 (1971).

[6] R. F. Casten, M. Wilhelm, E. Radermacher, N. V. Zamfir, and P. von Brentano, Phys. Rev**. C57**, R1553(R) (1998).

[7] K. Kumar and M. Baranger, Nucl. Phys. **A110**, 529 (1968).

[8] K. Kumar, Nucl. Phys. **A231**, 189 (1974).

[9]. F. Iachello and A. Arima, *The Interacting Boson Model* (Cambridge University Press, Cambridge, England 1987).

[10] O. Scholten, F. Iachello and A. Arima, Ann. Phys. (N.Y.) **115**, 325 (1978).

[11] F. Iachello, N.V. Zamfir and R.F. Casten, Phys. Rev. Lett. **81**, 061191 (1998).

[12] N.V. Zamfir, R.F. Casten, M.A. Caprio, C.W. Beausang, R. Krucken, J.R. Novak, J.R. Cooper, G. Cata Daniel and C.J. Barton, Phys. Rev. **C60**, 054312 (1999).

[13] W. D. Kulp *et al*. Phys. Rev. **C77**, 061301(R) (2008).

[14] J. B. Gupta, Phys. Rev. **C28**, 1929 (1983).

[15] O. Scholten, Computer program package PHINT KVI Internal Report, 1979.

[16] W.T. Chou, N.V. Zamfir and R.F. Casten, Phys. Rev. **C56**(02), 829 (1997).

[17] S. Hinds, J.H. Bjerregaard, O. Hansen and O. Nathan, Phys. Lett. **14**, 48 (1965).

[18] Jing-Ye Zhang, M.A. Caprio, N.V. Zamfir and R.F. Casten, Phys. Rev. **C60**, 061304 (1999).

[19] G. Gneuss and W. Greiner, Nucl. Phys. **A171**, 440 (1971).

[20] T. Klug, A Dewald, V. Werner, P. von Brentano and R.F. Casten, Phys. Lett. **B495**, 55 (2000).

[21] R.V. Jolos and P. von Brentano, Phys. Rev. **C80**, 034308 (2009).

[22] J.B. Gupta and J.H. Hamilton, Eur. Phys. J. **A51**, 151 (2015).

[23] J.B. Gupta, K. Kumar and J.H. Hamilton, Int. J. Mod. Phys. **E19**(07), 1491 (2010).

[24] N.V. Zamfir *et al*., Phys. Rev. **C65**, 067305 ((2002).

[25] R. Bijker, R.F. Casten, N.V. Zamfir and E.A. McCutchan, Phys. Rev. **C68**, 064310 (2003).

[26] W. McLatchie, J.E. Kitching and W. Darcey, Phys. Lett. **30B**, 529 (1969).

[27] P. Debenham and N.M. Hintz, Nucl. Phys. **A195**, 385 (1972).

[28] H. G. Borner *et al.*, Phys. Rev. **C73**, 034314 (2006).

[29] A.E.L. Dieperink, O, Scholten and F. Iachello, Phys. Rev. Lett. **44**, 1747 (1980).

[30] A.A. Shihab-Eldin, J.O. Rasmussen, M.A. Stoyer, D.G. Burke and P.E. Garrett, Int. J. Modern Phys. **E4**(2), 411 (1995).

[31] R. Fossion, C.E. Alanso, J.M. Arias, L. Fortunato and A. Vitturi, Phys. Rev. **C76**, 014316 (2007).

[32] Y. Zhang and F. Iachello, Phys. Rev. **C95**, 034306 (2017).

[33] R.M. Clark, R. F. Casten, L. Bettermann and R. Winkler, Phys. Rev. **C80**, 011303R (2009).

[34] L. Grodzins, Phys. Lett. **2**, 88 (1962).

[35] J.B. Gupta, Phys. Rev. **C89**, 034321(2014).

[36] J.B. Gupta, A.K. Kavathekar and R. Sharma, Phys. Scr. **51**, 316 (1995).

[37] H.M. Mittal, Vidya Thakur and J.B. Gupta, Phys. Scr. **81**, 015202 (2010).

[38] J.B. Gupta and A.K. Kavathekar, Pramana Jr. Phys. **61**, 167 (2003).

[39] R.F. Casten, N/V. Zamfir, P. von Brentano, F. Seiffert and W. Lieberz, Phys. Lett. **B265**, 9 (1991).

[40] N. Rud and K. Bonde Nielsen, Nucl. Phys. **A158**, 546 (1970).

[41] Jan Jolie, Pavel Cejnar and Jan Dobeš, Phys. Rev. **C60**, 061303 (1999).

[42] D.G. Burke, Phys. Rev. **C66**, 024312 (2002).

[43] R.M. Clark, M. Cromaz, M. A. Deleplanque, R.M. Diamond, P. Fallon, A. Görgen, I. Y. Lee, A. O. Macchiavelli, F.S. Stephens and D. Ward, Phys. Rev. **C67**, 041302R (2003).

[44] J.B. Gupta, Phys. Rev. **C33,** 1505 (1986).

[45] A. Arima and F. Iachello, Ann. Phys. **111**, 201 (1978).

[46] J.P. Elliot, Proc. Roy. Soc. Ser. **A245**, 128 (1958).

[47] J.B. Gupta and J.H. Hamilton, Phys. Rev. **C95**, 054303 (2017).

FIGURE CAPTIONS

FIG.1. Partial energy level spectrum of ^{152}Sm [3].

FIG. 2. Partial energy level spectrum of ^{152}Sm from DPPQ model.

FIG. 3. Potential energy curve for ^{152}Sm from DPPQ model. The zero point energy 'ZPE' lies 1.37 MeV below the spherical barrier.

FIG. 4. Variation of B($E2$, β-g) with ε/k in ^{152}Sm. The experimental values are shown by open circles.

FIG. 5. Variation of B(E2, γ-g, γ-β) with ε/k in ^{152}Sm. The experimental points are indicated by open circles.

FIG. 6. Partial energy spectrum of ^{152}Sm in IBM-1.

FIG. 7. The wave functions A_{100} and A_{200} for the 0_g and 0_β states of ^{152}Sm from DPPQ model.

FIG. 8. Partial ground band spectrum of ^{152}Sm in power index formula.

FIG. 9. The power index 'b' versus spin I for ^{152}Sm and ^{154}Gd.

FIG.10. Staggering index S(I) for N=88,90 and 92 in Sm, Gd and Dy.

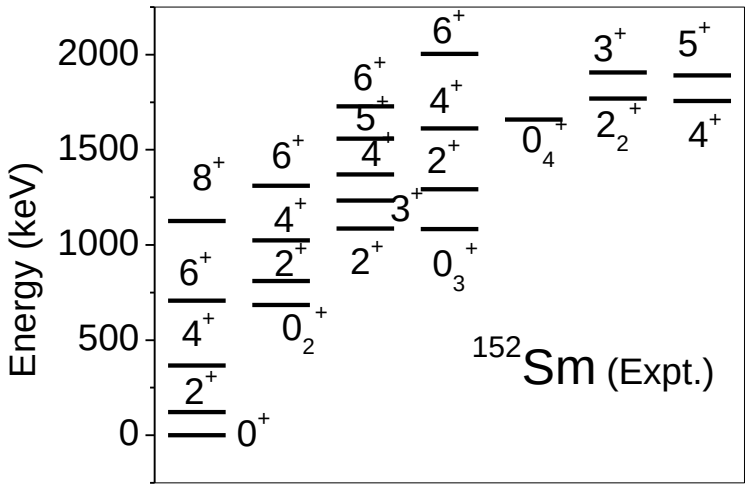

FIG.1. Partial energy level spectrum of ^{152}Sm [3].

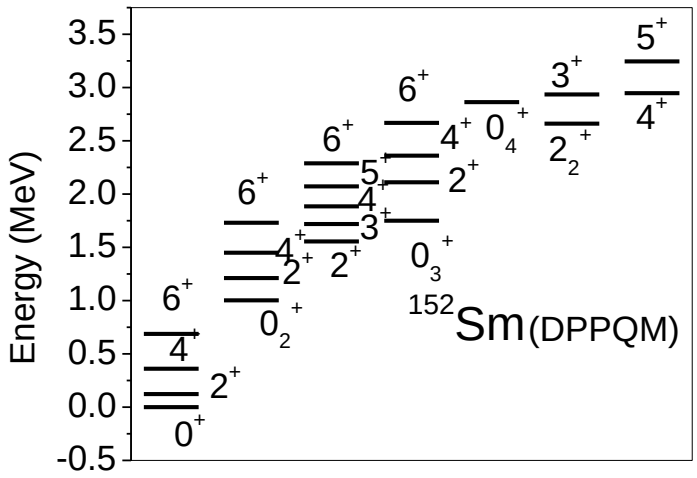

FIG. 2. Partial energy spectrum of ^{152}Sm from DPPQ model.

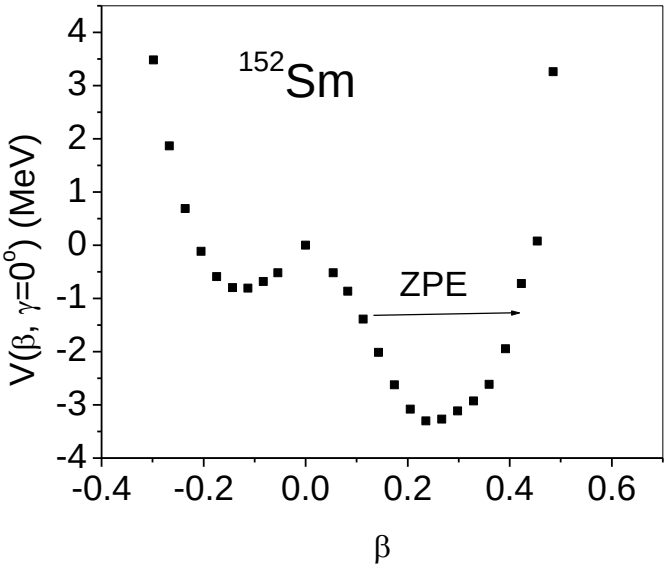

FIG. 3. Potential energy curve for ^{152}Sm from DPPQ model. The zero point energy 'ZPE' lies 1.37 MeV below the spherical barrier.

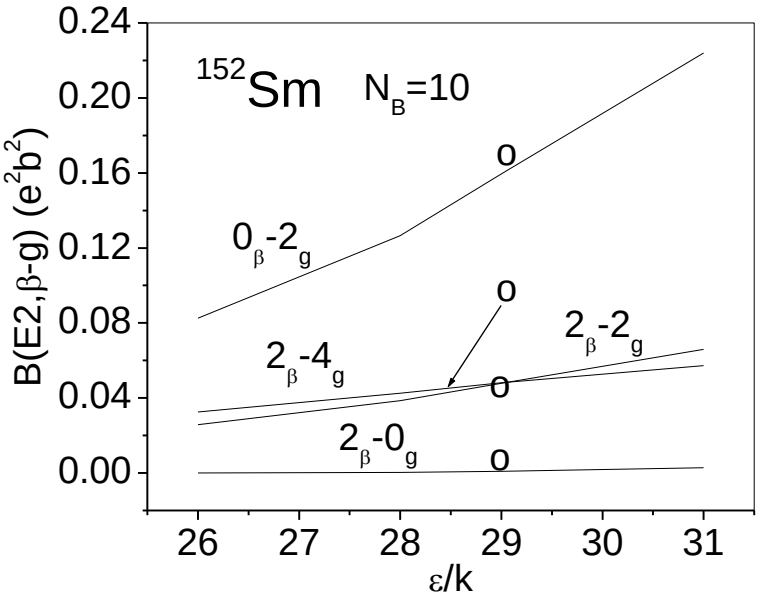

FIG. 4. Variation of B(E2, β-g) with ε/k. The experimental values are shown by open circle.

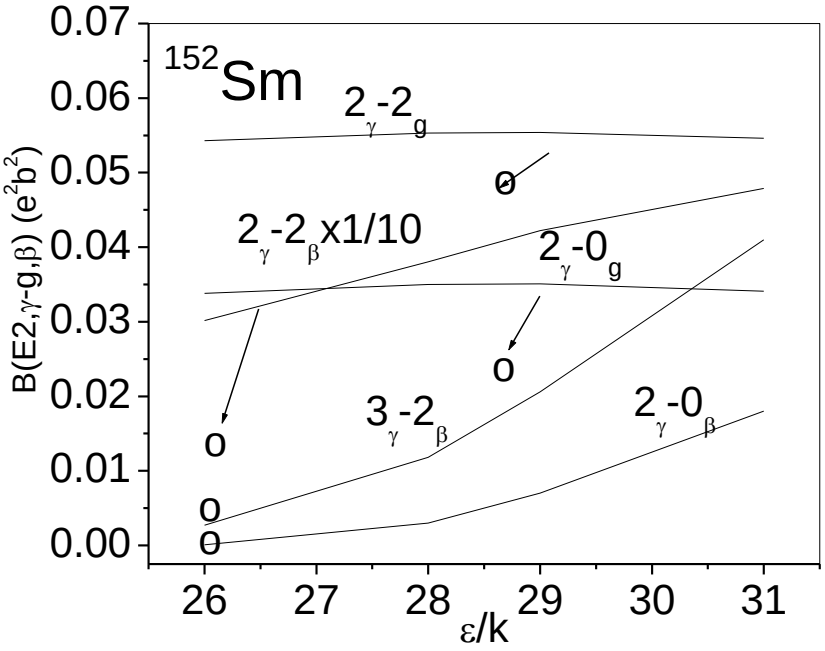

FIG. 5. Variation of B(E2, γ-g, γ-β) with ε/k in ^{152}Sm
The experimental points are indicated by open circles.

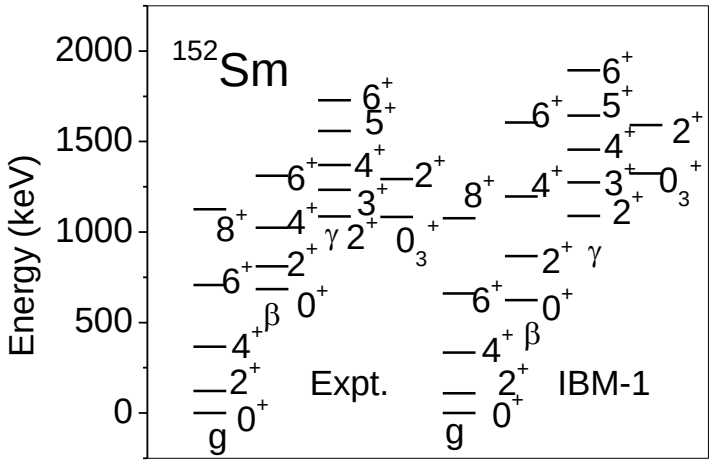

FIG. 6. Partial energy spectrum of ^{152}Sm in IBM-1.

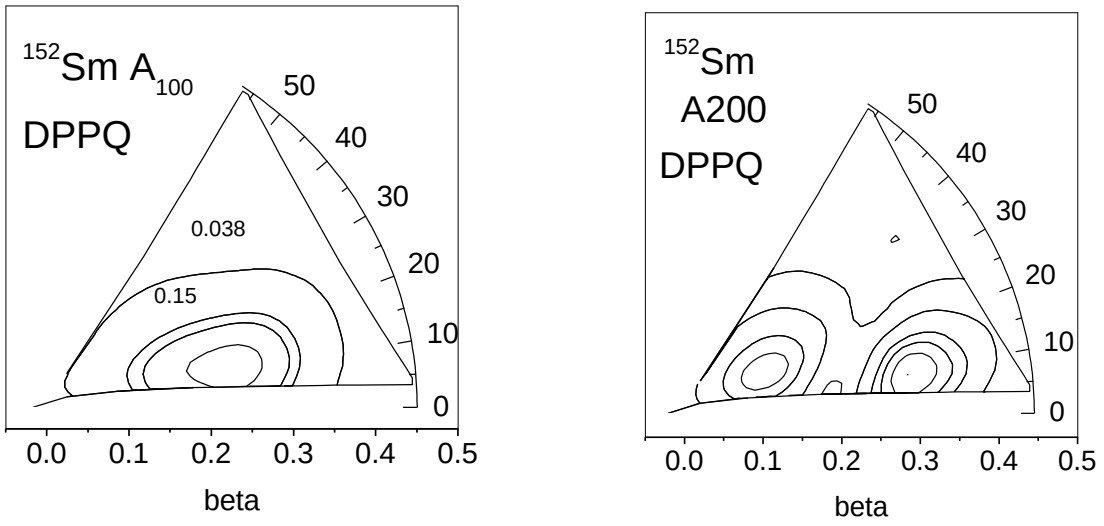

FIG. 7. The wave functions A_{100} and A_{200} for the 0_g and 0_β states of ^{152}Sm from DPPQ model.

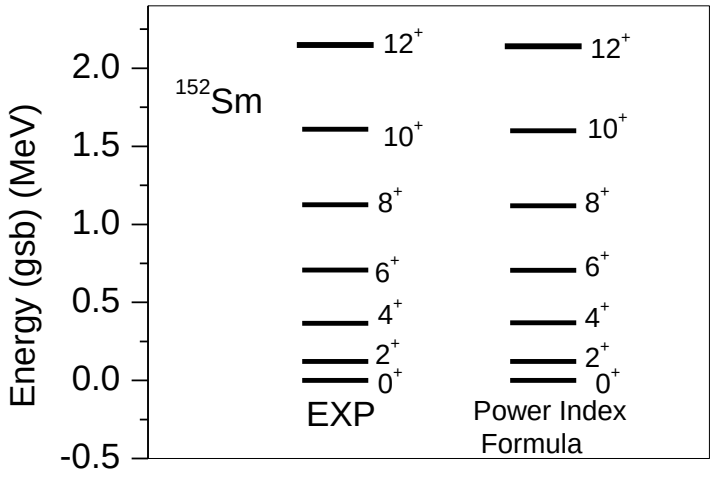

FIG. 8. Partial ground state band spectrum of ^{152}Sm in power index formula.

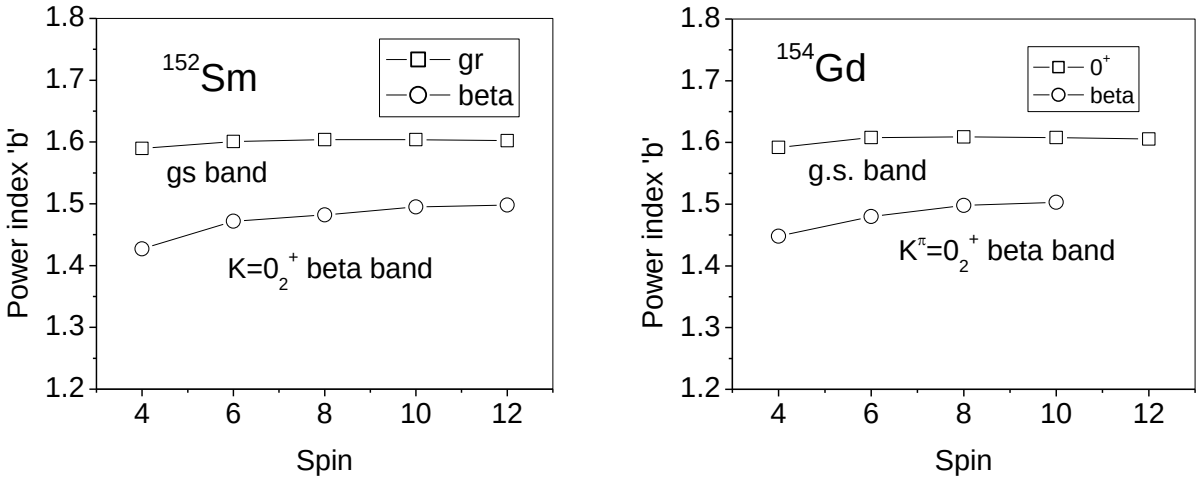

FIG. 9. Power index ‘b’ versus spin *I* for ^{152}Sm and ^{154}Gd.

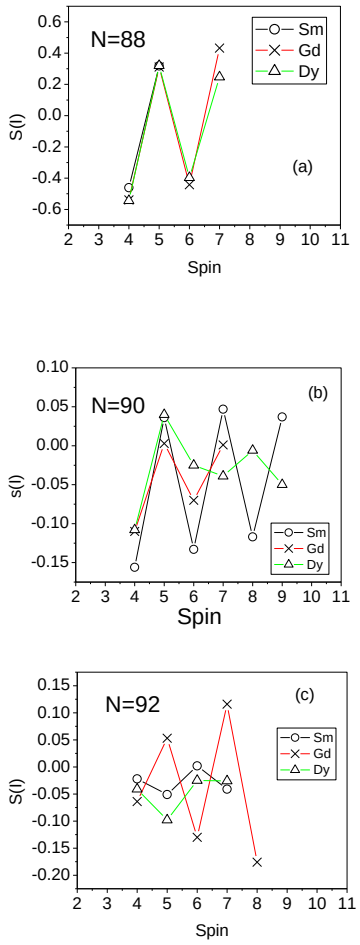

Fig. 10. Staggering index S(I) for *N*=88,90 and 92 in Sm, Gd and Dy.